

Cite this: *New J. Chem.*, 2019, 43, 709Received 17th October 2018,  
Accepted 23rd November 2018

DOI: 10.1039/c8nj05288c

rsc.li/njc

# Vilsmeier–Haack reagent mediated synthetic transformations with an immobilized iridium complex photoredox catalyst†

 Peng Zhi,<sup>‡a</sup> Zi-Wei Xi,<sup>‡a</sup> Dan-Yan Wang,<sup>‡b</sup> Wei Wang,<sup>c</sup> Xue-Zheng Liang,<sup>id \*a</sup>  
 Fei-Fei Tao,<sup>a</sup> Run-Pu Shen<sup>a</sup> and Yong-Miao Shen<sup>id \*ab</sup>

An immobilized iridium complex photocatalyst Ir(ppy)<sub>2</sub>(PDVB-py) was synthesized by immobilization of the iridium complex onto the nanoporous vinylpyridine-divinylbenzene copolymer (PDVB-py). Its application for the synthesis of amides, nitriles, and anhydrides was reported *via* reactions under the action of the visible-light-driven *in situ* generated Vilsmeier–Haack reagent from CBr<sub>4</sub> in DMF. The results showed that this heterogeneous photocatalyst has extremely high activity and excellent stability to be recycled five times.

## Introduction

The Vilsmeier–Haack reagent (halomethyleneiminium salt) is an efficient and mild electrophilic reagent, which has attracted great attention in synthetic organic chemistry.<sup>1</sup> Besides the general use in the formylation of aromatic and heteroaromatic compounds, it is now often used as one of the most common reagents in some interesting cyclisation reactions.<sup>2</sup> In addition, it also serves as an activating reagent in some functional group conversion reactions such as halogenation of alcohol and amidation of carboxylic acids.<sup>3</sup>

Vilsmeier–Haack reagent is usually formed *in situ* by the interaction of POCl<sub>3</sub> with *N,N*-disubstituted formamides (*e.g.*, *N,N*-dimethyl formamide, *N*-methyl formamide, *N*-formylpiperidine, and *N*-formylindoline).<sup>4</sup> Acid chlorides such as COCl<sub>2</sub>, SOCl<sub>2</sub>, CH<sub>3</sub>COCl, ArCOCl, ArSO<sub>2</sub>Cl, PCl<sub>5</sub>, *etc.* have also been used in the Vilsmeier reactions.<sup>5</sup>

Léonel reported a new Vilsmeier–Haack type reagent which was formed by the reduction of tetrahalomethanes (CCl<sub>4</sub> and CBr<sub>4</sub>) in dimethyl formamide (DMF) using superstoichiometric quantities of Fe and Cu powder.<sup>6</sup> However, these methods often require prior preparation of the reagents or harsh conditions and in some reactions stoichiometric additives are needed which generate stoichiometric waste by-products.

Visible-light photoredox catalysis has been established as a powerful and mild synthetic tool for the conversion of functional groups to construct complex organic molecules within the last decade. Various organic reactions with high synthetic value have been developed using ruthenium or iridium complexes as photocatalysts such as Ru(bpy)<sub>3</sub>Cl<sub>2</sub>, [Ir(ppy)<sub>2</sub>(dtbbpy)]<sup>+</sup>(PF<sub>6</sub><sup>−</sup>) or *fac*-Ir(ppy)<sub>3</sub>.<sup>7</sup>

Stephenson first reported a visible-light-mediated conversion of alcohols into halides with the Vilsmeier–Haack type reagent (CBr<sub>4</sub> in DMF) using only 1.0 mol% photoredox catalyst Ru(bpy)<sub>3</sub>Cl<sub>2</sub> instead of stoichiometric Fe and Cu powder.<sup>8</sup> Next, they successfully converted carboxylic acids into anhydrides using this protocol.<sup>9</sup> This protocol was subsequently applied to some other reactions. For example, the Yadav team efficiently converted aldoximes and primary amides into nitriles using eosin Y as the photocatalyst. They also achieved Beckmann rearrangement and Lossen rearrangement based on this synthetic strategy.<sup>10</sup> The Vilsmeier–Haack reagents could also be generated *in situ* under UVA irradiation. Barriault reported that carboxylic acids could be successfully converted into the corresponding anhydride and amide with the photogeneration of Vilsmeier–Haack reagents from DMF and CBr<sub>4</sub> with UVA light (365 nm LED).<sup>11</sup>

However, most reported visible-light-mediated reactions with Ir and Ru coordination compounds as photocatalysts use more than 1 mol% transition metal complex catalysts, and the catalysts are hard to recycle. This defect severely impeded their large-scale application. Hence, some attention has been paid to the synthesis of heterogeneous semiconductor photocatalysts<sup>12</sup> and immobilized Ir or Ru based complex photocatalysts, such as polyisobutylene (PIB)-polymer-tagged Ru complexes, polypyridyl iridium complex, *etc.* However, until now only a few examples of immobilized ruthenium and iridium-based photocatalysts have been reported.<sup>13</sup> The catalytic activity of the heterogeneous catalyst

<sup>a</sup> Key Laboratory of Clean Dyeing and Finishing Technology of Zhejiang Province, School of Chemistry and Chemical Engineering, Shaoxing University, Shaoxing, 312000, P. R. China

<sup>b</sup> Department of Chemistry, Zhejiang Sci-Tech University, Hangzhou, Zhejiang 310018, P. R. China. E-mail: shenym@zstu.edu.cn

<sup>c</sup> School of Civil Engineering, Shaoxing University, Shaoxing, 312000, P. R. China

† Electronic supplementary information (ESI) available. See DOI: 10.1039/c8nj05288c

‡ Peng Zhi, Zi-Wei Xi and Dan-Yan Wang contributed equally to this work.

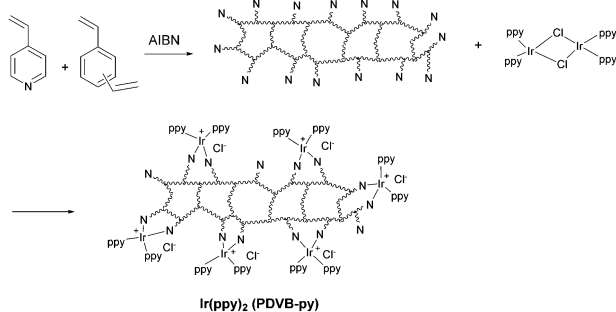
was greatly affected by the BET surface areas of the support. High surface areas of the support are highly demanded. The nano porous polydivinylbenzene (PDVB) was widely used as a support due to its high surface area and porosity,<sup>14</sup> and it could be easily used as an excellent solid chelating ligand *via* a simple copolymerization reaction. Recently, we have reported a novel supported iridium complex catalyst which was synthesized by the immobilization of iridium onto pyridine modified PDVB. This catalyst showed high catalytic activity and stability for the visible light mediated cyclization reaction of tertiary anilines with maleimides to give tetrahydroquinoline products.<sup>15</sup>

In the present work, we successfully applied these immobilized Ir complexes  $\text{Ir}(\text{ppy})_2(\text{PDVB-py})$  to the visible-light mediated *in situ* generation of the Vilsmeier–Haack type reagent for the synthesis of amides, nitriles and anhydrides in good to excellent yields. These Vilsmeier–Haack reagent mediated reactions could be easily scaled up and the immobilized iridium complex catalyst has a high turnover number and could be readily recycled more than five times.

## Results and discussion

First, we synthesized the highly active immobilized Ir complexes  $\text{Ir}(\text{ppy})_2(\text{PDVB-py})$  according to our previously published procedure (Scheme 1).<sup>15</sup> The scanning electron microscopy (SEM) image of  $\text{Ir}(\text{ppy})_2(\text{PDVB-py})$  exhibits irregular spherical structures (40–50 nm in diameter), which are quite similar to PDVB (Fig. 1). These small particles gathered to form clusters, which might be caused by the crosslinking of the Ir complexes. The energy dispersive spectrum (EDS) of  $\text{Ir}(\text{ppy})_2(\text{PDVB-py})$  showed evenly dispersed Ir in the polymer, indicating that iridium was successfully chelated to the copolymer. EDX gave a surface iridium content of 9.69 wt%, which was much higher than the value determined by ICP. This result indicates that most of the active iridium is dispersed on the surface, which is easily accessible to the reactants. The nitrogen content of the polymer was 7.83 wt%, which indicated abundant pyridine sites for chelating.

The N 1s XPS of  $\text{Ir}(\text{ppy})_2(\text{PDVB-py})$  showed the binding energy of N 1s was 400 eV, confirming that the pyridine species was present mainly at the chelating sites (Fig. 2). These results demonstrated the successful immobilization of Ir complexes



**Scheme 1** The synthetic route for the immobilized iridium complex photocatalyst.

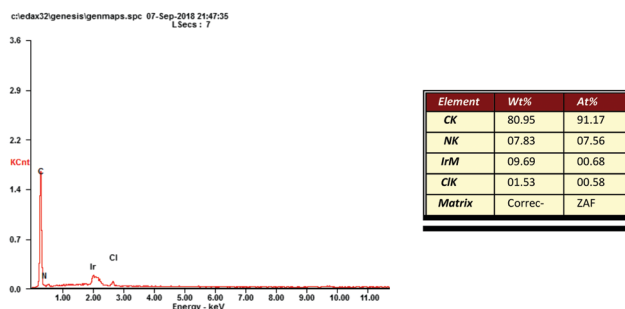
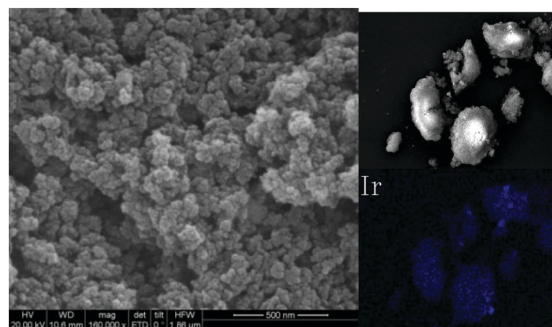


**Fig. 1** SEM-EDX images of  $\text{Ir}(\text{ppy})_2(\text{PDVB-py})$ .

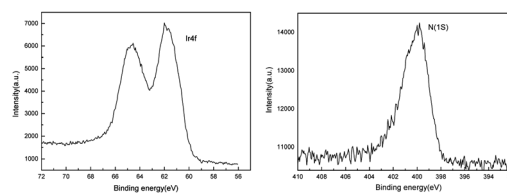


**Fig. 2** The N and Ir XPS spectra of  $\text{Ir}(\text{ppy})_2(\text{PDVB-py})$ .

onto the PDVB-py. Moreover, the iridium XPS spectra of  $\text{Ir}(\text{ppy})_2(\text{PDVB-py})$  showed that all the iridium element is present in the +3 oxidation state with binding energies of 61.5 and 64.5 eV in the Ir 4f<sub>7/2</sub> and Ir 4f<sub>5/2</sub> levels, respectively. The data agreed well with that of the control  $\text{Ir}(\text{ppy})_3$  complex. Thus, it could be concluded that the Ir complex was successfully immobilized on PDVB-py with a well-retained molecular configuration.

The nitrogen physisorption experiments were carried out (Fig. 3). The BET surface area of PDVB-py was 501 m<sup>2</sup> g<sup>-1</sup>, which could provide high surface areas for chelation and mass transfer. As to  $\text{Ir}(\text{ppy})_2(\text{PDVB-py})$ , the surface area greatly decreased to 85 m<sup>2</sup> g<sup>-1</sup>, which is accounted for by the bulky  $\text{Ir}(\text{ppy})_2$  moiety. The packed structure attached much importance to the high surface area. The nitrogen adsorption-desorption isotherm showed a typical curve, which indicated the mesoporous structure of the  $\text{Ir}(\text{ppy})_2(\text{PDVB-py})$ . The pore size was about 25 nm, which was suitable for the bulky reactants.

Initial studies concentrated on developing a procedure for the visible-light mediated Beckmann rearrangement through the Vilsmeier–Haack reagent. To our delight, we observed the formation of the desired Beckmann rearrangement reaction product in excellent yields using only 10 mg (iridium content is 0.4 mol% for **1a**)  $\text{Ir}(\text{ppy})_2(\text{PDVB-py})$  with acetonitrile (ACN) as

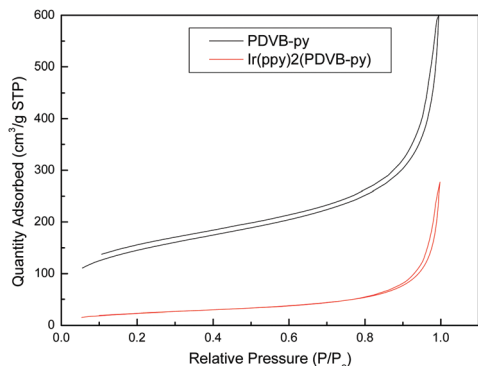


Fig. 3 The nitrogen sorption isotherms for Ir(ppy)<sub>2</sub>(PDVB-py) and PDVB-py.

Table 1 Optimization studies<sup>a</sup>

Entry	Solvent	Ir(ppy) <sub>2</sub> (PDVB-py) (mol%)	CBr <sub>4</sub> (equiv.)	Yield <sup>b</sup> 3a (%)
1	ACN	0.4	2	97.3
2	Acetone	0.4	2	21.3
3	CH <sub>2</sub> Cl <sub>2</sub>	0.4	2	47.6
4	NMP	0.4	2	13.0
5	THF	0.4	2	0.5
6	EtOH	0.4	2	0.2
7	ACN	0.8	2	97.4
8	ACN	0.2	2	97.0
9	ACN	0.4	1	85.2
10	ACN	0.4	1.5	89.6
11	ACN	0.4	2	0 <sup>c</sup>
12	ACN	0	2	0
13	ACN	0	2	90 <sup>d</sup>
14	ACN	0	2	18 <sup>e</sup>

<sup>a</sup> Reaction conditions: diphenyl ketoxime **1a** (1 mmol, 197 mg), Ir(ppy)<sub>2</sub>(PDVB-py), CBr<sub>4</sub> and DMF (20 mol%) in solvent (25 mL), purging with argon gas for 10 minutes, and then illumination by 3 W blue LED for 12 h.

<sup>b</sup> Determined by GC-MS. <sup>c</sup> Performed in the dark. <sup>d</sup> Catalyzed by *fac*-Ir(ppy)<sub>3</sub> (0.4 mol%) in isolated yield. <sup>e</sup> P25 (TiO<sub>2</sub>) (2 mol%) as the photocatalyst in isolated yield.

the solvent (Table 1, entry 1). The reaction could be catalyzed by *fac*-Ir(ppy)<sub>3</sub> (0.4 mol%) under the same optimized conditions to give an excellent isolated yield of 90% (Table 1, entry 13), while P25 (TiO<sub>2</sub>) was found to be ineffective in promoting this reaction (Table 1, entry 14).

The yields remained basically unchanged when we significantly increased or decreased the amount of the photocatalyst (Table 1, entries 7 and 8). This indicated that the dosage of catalyst could be further reduced, but for the convenience of weighing, we used 0.4 mol% of catalyst under the optimized reaction conditions. Control experiments confirmed that the presence of Ir(ppy)<sub>2</sub>(PDVB-py) and illumination was essential for the reaction to occur (Table 1, entries 11 and 12).

Next, we examined a series of substituted diphenyl ketoximes and acetophenone oximes under the optimized reaction

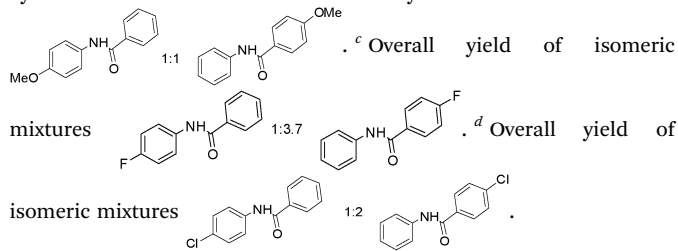
Table 2 Visible light mediated Beckmann rearrangement with Ir(ppy)<sub>2</sub>(PDVB-py) as the photocatalyst<sup>a</sup>

Entry	1	2	Yield (%)
1			95
2			93 <sup>b</sup>
3			91 <sup>c</sup>
4			89 <sup>d</sup>
5			92
6			91
7			90
8			91
9			94
10			94
11			75
12			90

Table 2 (continued)

Entry	1	2	Yield (%)
13			91
14			91

<sup>a</sup> General conditions: ketoxime **1** (1 mmol), Ir(ppy)<sub>2</sub>(PDVB-py) (0.4 mol%), CBr<sub>4</sub> (2 equiv.) and DMF (20 mol%) in ACN (25 mL), purging with argon gas for 10 minutes, and then illumination by 3 W blue LED for 12 h. <sup>b</sup> Overall yield of isomeric mixtures

Table 3 Optimization studies<sup>a</sup>

Entry	Solvent	Ir(ppy) <sub>2</sub> (PDVB-py) (mol%)	CBr <sub>4</sub> (equiv.)	Yield <b>4a</b> <sup>b</sup> (%)
1	ACN	0.8	2	84.5
2	Acetone	0.8	2	36.9
3	CH <sub>2</sub> Cl <sub>2</sub>	0.8	2	48.6
4	NMP	0.8	2	NT
5	THF	0.8	2	7.2
6	EtOH	0.8	2	12.6
7	ACN	1.5	2	88.9
8	ACN	0.4	2	81.9
9	ACN	0.8	2.5	89.1
10	ACN	0.8	1.5	82.9
11	ACN	0	2.5	92.7 <sup>c</sup>

<sup>a</sup> Reaction conditions: benzaldoxime (1 mmol), CBr<sub>4</sub>, Ir(ppy)<sub>2</sub>(PDVB-py) and DMF (20 mol%) in solvent (25 mL), purging with argon gas for 10 minutes, and then illumination by 3 W blue LED for 12 h. <sup>b</sup> Determined by GC-MS. <sup>c</sup> *fac*-Ir(ppy)<sub>3</sub> (0.8 mol%) as the photocatalyst.

conditions (Table 2). We found that for all substituted diphenyl ketoximes tested, the reactions proceeded with more than 89% yield irrespective of whether the substituent was electron-rich (entries 2 and 5) or electron-deficient (entries 3, 4, 6 and 7) on either of the phenyl rings (entry 1).

To further evaluate the catalytic performance of the immobilized iridium catalyst, we examined the conversion of aldoximes to nitriles under the action of the Vilsmeier-Haack reagent.

Table 4 Visible light mediated conversion of aldoximes to nitriles with Ir(ppy)<sub>2</sub>(PDVB-py) as the photocatalyst<sup>a</sup>

Entry	3	R <sup>1</sup>	R <sup>2</sup>	4	Yield (%)
1	<b>3a</b>	H	H	<b>4a</b>	80
2	<b>3b</b>	Me	H	<b>4b</b>	82
3	<b>3c</b>	OMe	H	<b>4c</b>	86
4	<b>3d</b>	CH(CH <sub>3</sub> ) <sub>2</sub>	H	<b>4d</b>	81
5	<b>3e</b>	C(CH <sub>3</sub> ) <sub>3</sub>	H	<b>4e</b>	84
6	<b>3f</b>	F	H	<b>4f</b>	75
7	<b>3g</b>	Cl	H	<b>4g</b>	70
8	<b>3h</b>	Me	Me	<b>4h</b>	81
9	<b>3i</b>	Ph	H	<b>4i</b>	87

<sup>a</sup> Reaction conditions: benzaldoxime (1 mmol), CBr<sub>4</sub> (2.5 equiv.), Ir(ppy)<sub>2</sub>(PDVB-py) (0.8 mol%) and DMF (20 mol%) in ACN (25 mL), purging with argon gas for 10 minutes, then illumination by 3 W blue LED.

Table 5 Optimization studies<sup>a</sup>

Entry	Solvent	Ir(ppy) <sub>2</sub> (PDVB-py) (mol%)	Base (equiv.)	Yield <b>6b</b> <sup>b</sup> (%)
1	ACN	0.4	<b>6a</b> (2)	86
2	CH <sub>2</sub> Cl <sub>2</sub>	0.4	<b>6a</b> (2)	80
3	ACN	0.4	<b>6a</b> (1.5)	76
4	ACN	0.4	<b>6a</b> (2.5)	82
5	ACN	0.4	<b>6b</b> (2)	35
7	ACN	0.4	<b>6c</b> (2)	65
8	ACN	0	<b>6a</b> (2)	0
9	ACN	0.4	<b>0</b>	0
10	ACN	0.4	<b>6a</b> (2)	0 <sup>c</sup>
11	ACN	0	<b>6a</b> (2)	86 <sup>d</sup>

**6a** (2,6-dimethylpyridine), **6b** (2,6-di-*tert*-butylpyridine), and **6c** (pyridine). <sup>a</sup> Reaction conditions: 4-methylbenzoic acid (1 mmol), CBr<sub>4</sub> (2 equiv.), Ir(ppy)<sub>2</sub>(PDVB-py), and DMF (20 mol%) base in solvent (25 mL), illumination by 3 W blue LED for 18 h. <sup>b</sup> Isolated yield. <sup>c</sup> Performed in the dark. <sup>d</sup> *fac*-Ir(ppy)<sub>3</sub> (0.4 mol%) as the photocatalyst.

We were delighted to find that visible-light irradiation (blue light-emitting diode (LED)) of benzaldoxime **3a** and CBr<sub>4</sub> (2.5 equiv.) in ACN in the presence of Ir(ppy)<sub>2</sub>(PDVB-py) (0.8 mol%) for 12 h furnished benzonitrile **4a** in 89% yield (Table 3, entry 9). Also we could get benzonitrile in an excellent yield of 93% with *fac*-Ir(ppy)<sub>3</sub> (0.8 mol%) as the photocatalyst.

The scope of the reaction under the optimized conditions was explored using a series of aldoximes (Table 4). We found that the reactions proceeded with more than 80% yield when the substituent was electron-rich on the aryl moiety, while the aryl with an electron withdrawing group appears to give relatively low yields (Table 2, entries 6 and 7).

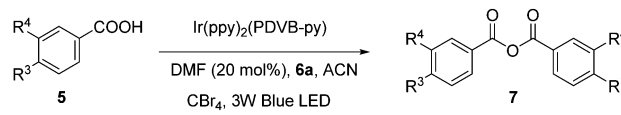
Furthermore, we investigated the application of the immobilized iridium complex in photocatalyzed anhydride synthesis from the corresponding carboxylic acid. 4-Methylbenzoic acid was used to optimize the reaction conditions. This reaction was

also found to proceed smoothly in the presence of Ir(ppy)<sub>2</sub>-(PDVB-py) to provide the desired *p*-methylbenzoic anhydride in good yield (Table 5, entry 1). We got the same isolated yield when we used *fac*-Ir(ppy)<sub>3</sub> (0.4 mol%) as the photocatalyst (Table 5, entry 11).

Further research has shown that the reactions proceeded well when there were electron-rich groups on the aryl moiety (Table 6, entries 1–4 and 6). The yield decreased noticeably when we used benzoic acid containing electron-withdrawing groups as the starting material (Table 6, entry 5). It turns out that the stability of the anhydride was the most important factor affecting the reaction yield. When the benzene ring contains a stronger electron-withdrawing group, such as CF<sub>3</sub>, F, *etc.*, we can detect the production of the anhydride product by GC-MS, but cannot get the separated product. Also, the decreased nucleophilicity of the acid greatly reduced the conversion of the starting material.

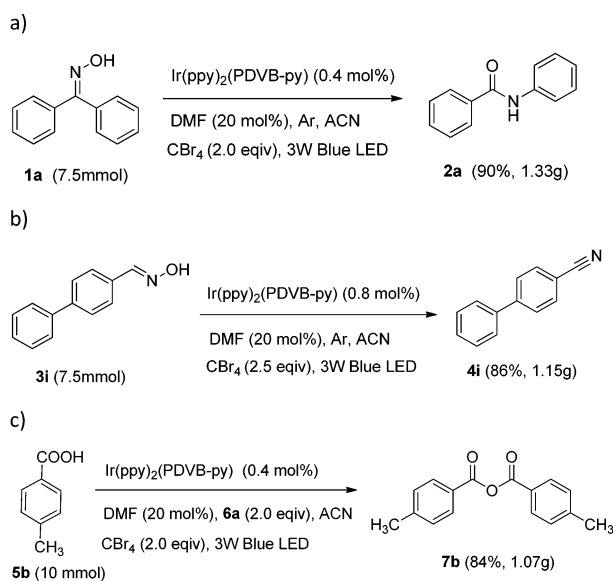
Gram-scale reactions were carried out for the above described transformations under optimized reaction conditions. We found

**Table 6** Visible light mediated conversion of carboxylic acids to the corresponding anhydrides with Ir(ppy)<sub>2</sub>(PDVB-py) as the photocatalyst<sup>a</sup>



Entry	5	R <sup>3</sup>	R <sup>4</sup>	7	Yield (%)
1	5a	H	H	7a	82
2	5b	Me	H	7b	86
3	5c	OMe	H	7c	86
4	5d	OMe	OMe	7d	83
5	5e	Cl	H	7e	71

<sup>a</sup> Reaction conditions: benzoic acid (1 mmol), CBr<sub>4</sub> (2 equiv.), Ir(ppy)<sub>2</sub>(PDVB-py) (0.4 mol%), DMF (20 mol%) and 6a (2 equiv.) in



**Scheme 2** Gram scale reactions.

ACN (25 mL), illumination by 3 W blue LED.

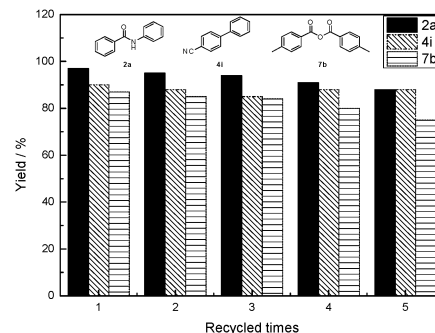


**Fig. 4** Supported catalyst Ir(ppy)<sub>2</sub>(PDVB-py) recycling in the visible-light mediated direct cyclization reaction.

that these reactions are easy to scale up and the yield is basically the same as that obtained in the corresponding small scale reaction (Scheme 2).

We then examined the recycling of the Ir(ppy)<sub>2</sub>(PDVB-py) photocatalyst. Experimentally, the catalyst is easily recovered from the reaction system by a simple centrifugal separation. The catalyst was then washed in alcohol and was reused without further treatment (Fig. 4). Remarkably, the results show that the photocatalyst could be efficiently recycled in five consecutive catalytic cycles without significant loss of reactivity and selectivity. The Ir-complex was attached to PDVB-py with two coordination bonds, which effectively prevents the active sites from releasing and guarantees the maintenance of the high catalytic activity. No iridium element was detected in the reaction solution and the washing solution by ICP-AES.

## Conclusions

In summary, we have developed new protocols for the synthesis of amides, nitriles and anhydrides using immobilized iridium complex photoredox catalysts in good to high chemical yield. Furthermore, the catalysts can be simply recycled and reused, which demonstrates that these environmentally friendly and economical protocols are improvements over previously reported procedures for similar types of reactions. Additionally, no change in the iridium content in the Ir(ppy)<sub>2</sub>(PDVB-py) catalyst was observed after the reaction.

## Experimental

All reagents were commercially available and used without further purification. All solvents were dried according to standard procedures. Melting points were measured on a Taikex-4 microscope melting point apparatus and were uncorrected. The <sup>1</sup>H and <sup>13</sup>C NMR spectra were recorded on a Bruker ACF-400 spectrometer at 400 and 100 MHz, respectively, using CDCl<sub>3</sub> and DMSO as solvents. SEM imaging was performed on a FEI Quanta 400 FEG microscope and EDS was performed on an EDAX Apollo XL system. XPS spectra were recorded on a Thermo ESCALAB 250XI. The Brunauer–Emmett–Teller (BET) surface area was measured using a Micromeritics Empyrean

instrument. GC-MS was carried out on an Agilent 59756890N. ICP-AES was carried out on a Leeman Prodigy XP instrument.

### General procedures for synthesis of amides, nitriles, and anhydrides

**Synthesis of amides.** A vial was charged with oxime (1 mmol),  $\text{CBr}_4$  (2 mmol),  $\text{Ir}(\text{ppy})_2(\text{PDVB-ppy})$  (0.4 mol%), and DMF (20 mol%) in ACN (25 mL). The vial was sealed and degassed with argon for 10 min. The reaction vessel was stirred 2 cm away from a 3 W blue LED and irradiated for 12 h. After centrifugal removal of catalyst, quenching with saturated aqueous sodium bicarbonate (30 mL) and extraction with ethyl acetate (30 mL), the organic phase was dried over anhydrous magnesium sulfate and evaporated to give a crude product. The crude mixture was purified by column chromatography on silica gel.

**Synthesis of nitriles.** A vial was charged with oxime (1 mmol),  $\text{CBr}_4$  (2.5 mmol),  $\text{Ir}(\text{ppy})_2(\text{PDVB-ppy})$  (0.8 mol%), and DMF (20 mol%) in ACN (25 mL). The vial was sealed and degassed with argon for 10 min. The reaction vessel was stirred 2 cm away from a 3 W blue LED and irradiated for 12 h. After centrifugal removal of catalyst, quenching with saturated aqueous sodium bicarbonate (30 mL) and extraction with ethyl acetate (30 mL), the organic phase was dried over anhydrous magnesium sulfate and evaporated to give a crude product. The crude mixture was purified by column chromatography on silica gel.

**Synthesis of anhydrides.** A vial was charged with acid (1 mmol),  $\text{CBr}_4$  (2 mmol),  $\text{Ir}(\text{ppy})_2(\text{PDVB-ppy})$  (0.4 mol%), DMF (20 mol%), and 2,6-dimethylpyridine (2 mmol) in ACN (25 mL). The reaction vessel was stirred 2 cm away from a 3 W blue LED and irradiated for 18 h. After centrifugal removal of catalyst, quenching with water and extraction with ethyl acetate (30 mL), the organic solvent was washed with saturated sodium bicarbonate (15 mL) and NaCl solution (15 mL), dried over anhydrous magnesium sulfate and evaporated to give a crude product. The crude mixture was purified by column chromatography on silica gel.

**Supported catalyst  $\text{Ir}(\text{ppy})_2(\text{PDVB-ppy})$  recycling.** The catalyst was centrifuged in the reaction solution, washed with ethanol, and then used after drying.

*N*-Phenylbenzamide (**2a**). White solid [white solid], m.p. 160–162 °C [163–164 °C],<sup>16</sup> 95% (187 mg). <sup>1</sup>H NMR (400 MHz,  $\text{CDCl}_3$ )  $\delta$  7.86 (d, 3H,  $J = 7.6$  Hz), 7.64 (d, 2H,  $J = 7.6$  Hz), 7.56–7.53 (m, 1H), 7.50–7.46 (m, 2H), 7.37 (t, 2H,  $J = 7.4$  Hz), 7.15 (t, 1H,  $J = 7.2$  Hz). <sup>13</sup>C NMR (100 MHz,  $\text{CDCl}_3$ )  $\delta$  165.8, 137.9, 135.0, 131.9, 129.1, 128.8, 127.0, 124.6, 120.2.

*N*-(4-Methoxyphenyl)benzamide: 4-methoxy-*N*-phenylbenzamide = 1:1 (**2b**). White solid [white solid], m.p. 146–163 °C [148–161 °C],<sup>17</sup> 93% (211 mg). <sup>1</sup>H NMR (400 MHz,  $\text{CDCl}_3$ )  $\delta$  7.87–7.82 (m, 4.32H), 7.78 (s, 1.65H), 7.63 (d, 1.75H,  $J = 8.0$  Hz), 7.55–7.53 (m, 3.32H), 7.50–7.45 (m, 2.37H), 7.37 (t, 1.67H,  $J = 7.8$  Hz), 7.14 (t, 0.86H,  $J = 7.4$  Hz), 6.98–6.95 (m, 1.98H), 6.91 (d, 2.01H,  $J = 8.8$  Hz), 3.87 (s, 2.95H), 3.82 (s, 3H). <sup>13</sup>C NMR (100 MHz,  $\text{CDCl}_3$ )  $\delta$  162.5, 156.6, 138.1, 135.0, 132.0, 131.7, 130.9, 129.1,

128.9, 128.8, 127.0, 124.4, 122.1, 121.7, 120.1, 114.2, 114.0, 55.5, 55.4.

*N*-(4-Fluorophenyl)benzamide: 4-fluoro-*N*-phenylbenzamide = 1:3.7 (**2c**). White solid [off-white solid], m.p. 168–178 °C [167–178 °C],<sup>17</sup> 91% (196 mg). <sup>1</sup>H NMR (400 MHz,  $\text{CDCl}_3$ )  $\delta$  7.91–7.86 (m, 2.75H), 7.78 (s, 0.35H), 7.74 (s, 0.6H), 7.62 (d, 2.38H,  $J = 7.6$  Hz), 7.60–7.55 (m, 0.8H), 7.50 (t, 0.78H,  $J = 7.4$  Hz), 7.38 (t, 2H,  $J = 7.9$  Hz), 7.21–7.13 (m, 3.19H), 7.07 (t, 0.87H,  $J = 8.6$  Hz). <sup>13</sup>C NMR (100 MHz,  $\text{CDCl}_3$ )  $\delta$  166.2, 165.7, 164.7, 163.7, 158.4, 137.8, 134.7, 133.9 (d,  $J = 2.8$  Hz), 132.0, 131.1 (d,  $J = 3.0$  Hz), 129.4 (d,  $J = 8.9$  Hz), 129.2, 128.8, 127.0, 124.7, 122.1 (d,  $J = 7.8$  Hz), 120.3, 115.9 (d,  $J = 22.0$  Hz), 115.8 (d,  $J = 22.0$  Hz).

4-Chloro-*N*-phenylbenzamide (**2da**). White solid [white solid], m.p. 199–200 °C [200–201 °C],<sup>18</sup> 60% (137 mg). <sup>1</sup>H NMR (400 MHz, DMSO)  $\delta$  10.31 (s, 1H), 8.03–7.94 (m, 2H), 7.78–7.76 (m, 2H), 7.64–7.58 (m, 2H), 7.39–7.32 (m, 2H), 7.15–7.07 (m, 1H). <sup>13</sup>C NMR (100 MHz, DMSO)  $\delta$  164.9, 139.4, 136.8, 134.1, 130.1, 129.1, 128.9, 124.3, 120.9.

*N*-(4-Chlorophenyl)benzamide: 4-chloro-*N*-phenylbenzamide = 1:2 (**2d**). White solid, m.p. 185–197 °C, 89% (206 mg). <sup>1</sup>H NMR (400 MHz,  $\text{CDCl}_3$ )  $\delta$  7.89–7.84 (m, 1.07H), 7.84–7.80 (m, 2.33H), 7.78 (s, 0.70H), 7.62 (t, 3H,  $J = 7.9$  Hz), 7.57 (t, 0.52H,  $J = 4.9$  Hz), 7.51 (d, 0.98H,  $J = 7.8$  Hz), 7.49–7.45 (m, 2.17H), 7.41–7.36 (m, 2.02H), 7.36–7.32 (m, 1.02H), 7.18 (t, 1.02H,  $J = 7.4$  Hz). <sup>13</sup>C NMR (100 MHz,  $\text{CDCl}_3$ )  $\delta$  165.7, 164.6, 138.2, 137.7, 136.5, 134.7, 133.4, 132.1, 129.6, 129.2, 129.14, 129.08, 128.9, 128.5, 127.0, 124.8, 121.4, 120.3.

4-Methyl-*N*-(*p*-tolyl)benzamide (**2e**). White solid [white solid], m.p. 212–213 °C [210–211 °C],<sup>16</sup> 92% (207 mg). <sup>1</sup>H NMR (400 MHz, DMSO)  $\delta$  10.09 (s, 1H), 7.87 (d, 2H,  $J = 8.1$  Hz), 7.66 (d, 2H,  $J = 8.4$  Hz), 7.33 (d, 2H,  $J = 8.0$  Hz), 7.15 (d, 2H,  $J = 8.3$  Hz), 2.38 (s, 3H), 2.28 (s, 3H). <sup>13</sup>C NMR (100 MHz, DMSO)  $\delta$  165.6, 141.9, 137.2, 132.9, 132.6, 129.4, 129.3, 128.1, 120.8, 21.5, 21.0.

4-Fluoro-*N*-(4-fluorophenyl)benzamide (**2f**). White solid [white solid], m.p. 178–180 °C [180–181 °C],<sup>16</sup> 91% (212 mg). <sup>1</sup>H NMR (400 MHz, DMSO)  $\delta$  10.32 (s, 1H), 8.10–7.97 (m, 2H), 7.86–7.70 (m, 2H), 7.38 (t, 2H,  $J = 8.8$  Hz), 7.25–7.14 (m, 2H). <sup>13</sup>C NMR (100 MHz, DMSO)  $\delta$  164.5 (d,  $J = 247.5$  Hz), 164.8, 158.8 (d,  $J = 238.7$  Hz), 135.9 (d,  $J = 2.7$  Hz), 131.7 (d,  $J = 2.8$  Hz), 130.8 (d,  $J = 8.9$  Hz), 122.7 (d,  $J = 7.7$  Hz), 115.8 (d,  $J = 22.0$  Hz), 115.6 (d,  $J = 22.0$  Hz).

4-Chloro-*N*-(4-chlorophenyl)benzamide (**2g**). White solid [white solid], m.p. 202–203 °C [202–203 °C],<sup>16</sup> 90% (240 mg). <sup>1</sup>H NMR (400 MHz,  $\text{CDCl}_3$ )  $\delta$  7.81 (d, 2H,  $J = 8.4$  Hz), 7.75 (s, 1H), 7.59 (d, 2H,  $J = 8.7$  Hz), 7.47 (d, 2H,  $J = 8.4$  Hz), 7.34 (d, 2H,  $J = 8.6$  Hz). <sup>13</sup>C NMR (100 MHz,  $\text{CDCl}_3$ )  $\delta$  164.6, 138.4, 136.2, 133.0, 129.8, 129.19, 129.15, 128.4, 121.5.

*N*-Phenylacetamide (**2h**). White solid [white solid], m.p. 112–115 °C [114–116 °C],<sup>17</sup> 91% (123 mg). <sup>1</sup>H NMR (400 MHz,  $\text{CDCl}_3$ )  $\delta$  7.61 (s, 1H), 7.50 (d, 2H,  $J = 7.7$  Hz), 7.31 (t, 2H,  $J = 7.9$  Hz), 7.10

(t, 1H,  $J = 7.4$  Hz), 2.17 (s, 3H).  $^{13}\text{C}$  NMR (100 MHz,  $\text{CDCl}_3$ )  $\delta$  168.6, 137.8, 129.0, 124.4, 120.0, 24.5.

*N*-(*p*-Tolyl)acetamide (**2i**). White solid [off-white solid], m.p. 146–147 °C [149–151 °C],<sup>17</sup> 94% (140 mg).  $^1\text{H}$  NMR (400 MHz,  $\text{CDCl}_3$ )  $\delta$  7.37 (d, 2H,  $J = 8.4$  Hz), 7.23 (s, 1H), 7.12 (d, 2H,  $J = 8.2$  Hz), 2.31 (s, 3H), 2.17 (s, 3H).  $^{13}\text{C}$  NMR (100 MHz,  $\text{CDCl}_3$ )  $\delta$  168.3, 135.2, 134.0, 129.5, 120.0, 24.5, 20.9.

*N*-(4-Methoxyphenyl)acetamide (**2j**). White solid [light-brown], m.p. 128–130 °C [129–130 °C],<sup>17</sup> 94% (155 mg).  $^1\text{H}$  NMR (400 MHz,  $\text{CDCl}_3$ )  $\delta$  7.42–7.36 (m, 2H), 7.35 (s, 1H), 6.88–6.82 (m, 2H), 3.79 (s, 3H), 2.16 (s, 3H).  $^{13}\text{C}$  NMR (100 MHz,  $\text{CDCl}_3$ )  $\delta$  168.4, 156.5, 130.8, 122.0, 114.1, 55.5, 24.3.

*N*-(4-Fluorophenyl)acetamide (**2k**). White solid [colorless needle], m.p. 149–152 °C [152–153 °C],<sup>19</sup> 75% (115 mg).  $^1\text{H}$  NMR (400 MHz,  $\text{CDCl}_3$ )  $\delta$  7.50–7.41 (m, 3H), 7.04–6.96 (m, 2H), 2.17 (s, 3H).  $^{13}\text{C}$  NMR (100 MHz,  $\text{CDCl}_3$ )  $\delta$  168.4, 159.4 (d,  $J = 242.3$  Hz), 133.8, 121.8 (d,  $J = 7.9$  Hz), 115.6 (d,  $J = 22.3$  Hz), 24.4.

*N*-(4-Chlorophenyl)acetamide (**2l**). White solid [white solid], m.p. 178–181 °C [177–181 °C],<sup>20</sup> 90% (153 mg).  $^1\text{H}$  NMR (400 MHz,  $\text{CDCl}_3$ )  $\delta$  7.46 (d, 2H,  $J = 8.8$  Hz), 7.28 (d, 2H,  $J = 8.8$  Hz), 7.21 (s, 1H), 2.19 (s, 3H).  $^{13}\text{C}$  NMR (100 MHz,  $\text{CDCl}_3$ )  $\delta$  168.3, 136.4, 129.3, 129.0, 121.0, 24.6.

*N*-Benzylacetamide (**2m**). White solid [pale-yellow solid], m.p. 102–103 °C [103–104 °C],<sup>17</sup> 91% (136 mg).  $^1\text{H}$  NMR (400 MHz,  $\text{CDCl}_3$ )  $\delta$  8.19 (s, 1H), 7.52 (d, 2H,  $J = 7.8$  Hz), 7.26 (t, 2H,  $J = 7.9$  Hz), 7.06 (t, 1H,  $J = 7.4$  Hz), 2.35 (q, 2H,  $J = 7.6$  Hz), 1.19 (t, 3H,  $J = 7.6$  Hz).  $^{13}\text{C}$  NMR (100 MHz,  $\text{CDCl}_3$ )  $\delta$  172.9, 138.2, 128.9, 124.1, 120.2, 30.6, 9.8.

*N*-([1,1'-Biphenyl]-4-yl)acetamide (**2n**). White solid [colorless solid], m.p. 170–173 °C [171–172 °C],<sup>21</sup> 91% (192 mg).  $^1\text{H}$  NMR (400 MHz,  $\text{CDCl}_3$ )  $\delta$  7.68 (s, 1H), 7.60–7.52 (m, 6H), 7.42 (t, 2H,  $J = 7.6$  Hz), 7.32 (t, 1H,  $J = 7.3$  Hz), 2.19 (s, 3H).  $^{13}\text{C}$  NMR (100 MHz,  $\text{CDCl}_3$ )  $\delta$  168.6, 140.4, 137.2, 137.1, 128.8, 127.6, 127.1, 126.8, 120.3, 24.6.

*Benzonitrile* (**4a**). Colorless liquid [colorless oil],<sup>22</sup> 80% (82 mg).  $^1\text{H}$  NMR (400 MHz,  $\text{CDCl}_3$ )  $\delta$  7.68–7.59 (m, 3H), 7.48 (t, 2H,  $J = 7.8$  Hz).  $^{13}\text{C}$  NMR (100 MHz,  $\text{CDCl}_3$ )  $\delta$  132.8, 132.1, 129.2, 118.9, 112.4.

*4*-Methylbenzonitrile (**4b**). Colorless liquid [yellow liquid],<sup>22</sup> 82% (96 mg).  $^1\text{H}$  NMR (400 MHz,  $\text{CDCl}_3$ )  $\delta$  7.52 (d, 2H,  $J = 8.0$  Hz), 7.28–7.25 (m, 2H), 2.42 (s, 3H).  $^{13}\text{C}$  NMR (100 MHz,  $\text{CDCl}_3$ )  $\delta$  143.7, 132.0, 129.8, 119.2, 109.3, 21.8.

*4*-Methoxybenzonitrile (**4c**). White solid [yellow solid], m.p. 60–61 °C [61–62 °C],<sup>22</sup> 86% (115 mg).  $^1\text{H}$  NMR (400 MHz,  $\text{CDCl}_3$ )  $\delta$  7.69–7.41 (m, 2H), 7.02–6.88 (m, 2H), 3.86 (s, 3H).  $^{13}\text{C}$  NMR (100 MHz,  $\text{CDCl}_3$ )  $\delta$  162.8, 134.0, 119.2, 114.8, 103.9, 55.6.

*4*-Isopropylbenzonitrile (**4d**). Colorless liquid [colorless oil],<sup>24</sup> 81% (118 mg).  $^1\text{H}$  NMR (400 MHz,  $\text{CDCl}_3$ )  $\delta$  7.60–7.53 (m, 2H), 7.32 (d, 2H,  $J = 8.3$  Hz), 3.00–2.93 (m, 1H), 1.26 (d, 6H,  $J = 6.9$  Hz).

$^{13}\text{C}$  NMR (100 MHz,  $\text{CDCl}_3$ )  $\delta$  154.4, 132.2, 127.3, 119.2, 109.6, 34.4, 23.5.

*4*-(*tert*-Butyl)benzonitrile (**4e**). Colorless liquid [oil],<sup>25</sup> 84% (134 mg).  $^1\text{H}$  NMR (400 MHz,  $\text{CDCl}_3$ )  $\delta$  7.58 (d, 2H,  $J = 8.3$  Hz), 7.48 (d, 2H,  $J = 8.5$  Hz), 1.33 (s, 9H).  $^{13}\text{C}$  NMR (100 MHz,  $\text{CDCl}_3$ )  $\delta$  156.6, 131.9, 126.2, 119.1, 109.3, 35.2, 30.9.

*4*-Fluorobenzonitrile (**4f**). White solid [yellow solid], m.p. 31–32 °C [29–31 °C],<sup>22</sup> 75% (91 mg).  $^1\text{H}$  NMR (400 MHz,  $\text{CDCl}_3$ )  $\delta$  7.72–7.66 (m, 2H), 7.22–7.15 (m, 2H).  $^{13}\text{C}$  NMR (100 MHz,  $\text{CDCl}_3$ )  $\delta$  165.1 (d,  $J = 255.5$  Hz), 134.7 (d,  $J = 9.1$  Hz), 118.0, 116.9 (d,  $J = 22.5$  Hz), 108.6 (d,  $J = 3.6$  Hz).

*4*-Chlorobenzonitrile (**4g**). White solid [yellow solid], m.p. 89–91 °C [91–93 °C],<sup>22</sup> 70% (96 mg).  $^1\text{H}$  NMR (400 MHz,  $\text{CDCl}_3$ )  $\delta$  7.69–7.57 (m, 2H), 7.52–7.43 (m, 2H).  $^{13}\text{C}$  NMR (100 MHz,  $\text{CDCl}_3$ )  $\delta$  139.5, 133.4, 129.7, 118.0, 110.8.

*3,4*-Dimethylbenzonitrile (**4h**). White solid, m.p. 66–67 °C [63–64 °C],<sup>23</sup> 81% (106 mg).  $^1\text{H}$  NMR (400 MHz,  $\text{CDCl}_3$ )  $\delta$  7.42–7.37 (m, 2H), 7.22 (d, 1H,  $J = 7.7$  Hz), 2.32 (s, 3H), 2.29 (s, 3H).  $^{13}\text{C}$  NMR (100 MHz,  $\text{CDCl}_3$ )  $\delta$  142.5, 137.9, 132.8, 130.3, 129.6, 119.3, 109.5, 20.2, 19.6.

[1,1'-Biphenyl]-4-carbonitrile (**4i**). White solid [yellow solid], m.p. 83–85 °C [85–87 °C],<sup>22</sup> 87% (156 mg).  $^1\text{H}$  NMR (400 MHz,  $\text{CDCl}_3$ )  $\delta$  7.75–7.67 (m, 4H), 7.60–7.58 (m, 2H), 7.51–7.46 (m, 2H), 7.45–7.40 (m, 1H).  $^{13}\text{C}$  NMR (100 MHz,  $\text{CDCl}_3$ )  $\delta$  145.7, 139.2, 132.6, 129.1, 128.7, 127.7, 127.2, 118.9, 110.9.

*Benzoic anhydride* (**7a**). White solid [light yellow solid], m.p. 40–41 °C [39–41 °C],<sup>25</sup> 82% (93 mg).  $^1\text{H}$  NMR (400 MHz,  $\text{CDCl}_3$ )  $\delta$  8.18–8.15 (m, 4H), 7.67–7.65 (m, 2H), 7.54–7.51 (m, 4H).  $^{13}\text{C}$  NMR (100 MHz,  $\text{CDCl}_3$ )  $\delta$  162.4, 134.6, 130.6, 128.9, 128.8.

*4*-Methylbenzoic anhydride (**7b**). White solid [light yellow solid], m.p. 87–89 °C [88–89 °C],<sup>25</sup> 86% (109 mg).  $^1\text{H}$  NMR (400 MHz,  $\text{CDCl}_3$ )  $\delta$  8.04 (d, 4H,  $J = 8.3$  Hz), 7.32 (d, 4H,  $J = 8.0$  Hz), 2.46 (s, 6H).  $^{13}\text{C}$  NMR (100 MHz,  $\text{CDCl}_3$ )  $\delta$  162.6, 145.6, 130.6, 129.6, 126.2, 21.9.

*4*-Methoxybenzoic anhydride (**7c**). White solid [light yellow solid], m.p. 90–91 °C [89–90 °C],<sup>26</sup> 86% (123 mg).  $^1\text{H}$  NMR (400 MHz, DMSO)  $\delta$  8.11–8.03 (m, 4H), 7.18–7.11 (m, 4H), 3.89 (s, 6H).  $^{13}\text{C}$  NMR (100 MHz, DMSO)  $\delta$  165.0, 162.6, 133.2, 120.6, 115.1, 56.3.

*3,4*-Dimethoxybenzoic anhydride (**7d**). White solid, m.p. 123–125 °C [124–125 °C],<sup>27</sup> 83% (144 mg).  $^1\text{H}$  NMR (400 MHz, DMSO)  $\delta$  7.77 (dd, 2H,  $J = 8.5, 2.0$  Hz), 7.56 (d, 2H,  $J = 2.0$  Hz), 7.16 (d, 2H,  $J = 8.6$  Hz), 3.89 (s, 6H), 3.86 (s, 6H).  $^{13}\text{C}$  NMR (100 MHz, DMSO)  $\delta$  162.8, 154.9, 149.3, 125.5, 120.6, 112.7, 111.9, 56.4, 56.1.

*4*-Chlorobenzoic anhydride (**7e**). White solid [yellow solid], m.p. 183–185 °C [184–185 °C],<sup>26</sup> 71% (105 mg).  $^1\text{H}$  NMR (400 MHz,  $\text{CDCl}_3$ )  $\delta$  8.08 (d, 4H,  $J = 8.6$  Hz), 7.52 (d, 4H,  $J = 8.5$  Hz).  $^{13}\text{C}$  NMR (100 MHz,  $\text{CDCl}_3$ )  $\delta$  161.3, 141.4, 131.9, 129.4, 127.1.

## Conflicts of interest

There are no conflicts to declare.

## Acknowledgements

This work was supported by the National Natural Science Foundation of China (NSFC 21202101 and 41772311), Zhejiang Provincial Natural Science Foundation (LY16B020006), China Postdoctoral Science Foundation (2015M581919) and Science Foundation of Zhejiang Sci-Tech University (18062144-Y).

## Notes and references

- (a) B. Meenu and J. Neelam, *Eur. J. Biomed. Pharm. Sci.*, 2015, **2**, 1340–1374; (b) A. Vilsmeier and A. Haack, *Ber. Dtsch. Chem. Ges. A*, 1927, **60**, 119–122; (c) J.-P. Lellouche and V. Kotlya, *Synlett*, 2004, 564–571; (d) A. P. Rajput and P. D. Girase, *Int. J. Pharm., Chem. Biol. Sci.*, 2012, **3**, 25–43; (e) R. K. Pardeshiet, *Heterocycl. Lett.*, 2015, **5**, 629–635.
- (a) C. Allais, J. M. Grassot, J. Rodriguez and T. Constantieux, *Chem. Rev.*, 2014, **114**, 10829–10868; (b) O. Meth-Cohn and D. L. Taylor, *J. Chem. Soc., Chem. Commun.*, 1995, 1463–1464; (c) A. Jackson and O. Meth-Cohn, *J. Chem. Soc., Chem. Commun.*, 1995, 1319; (d) B. Muddam, P. Venkanna, M. Venkateswarlu, M. S. Kumar and K. C. Rajanna, *Synlett*, 2018, 85–88; (e) C. Sandoval, N. K. Lim and H. Zhang, *Org. Lett.*, 2018, **20**, 1252–1255; (f) M. Bhat, G. K. Nagaraja, R. Kayarmar and S. K. Peethamber, *RSC Adv.*, 2016, **6**, 59375–59388.
- (a) W. Su, Y. Weng, L. Jiang, Y. Yang, L. Zhao, Z. Chen and J. Li, *Org. Prep. Proced. Int.*, 2010, **42**, 503–555; (b) S. Selvi and P. T. Perumal, *Org. Prep. Proced. Int.*, 2001, **33**, 194–198; (c) P. A. Procopiou, A. C. Brodie, M. J. Deal and D. F. Hayman, *J. Chem. Soc., Perkin Trans. 1*, 1996, 2249.
- (a) A. P. Rajput and P. D. Girase, *Int. J. Pharm. Pharm. Sci.*, 2011, **3**, 214; (b) V. I. Minkin and G. N. Dorofeenko, *Russ. Chem. Rev.*, 1960, **29**, 599; (c) P. Thamyongkit, A. D. Bhise, M. Taniguchi and J. S. Lindsey, *J. Org. Chem.*, 2006, **71**, 903–910.
- (a) B. A. J. Clark, J. Parrick, P. J. West and A. H. Kelly, *J. Chem. Soc.*, 1970, 498–501; (b) F. L. Scott and J. A. Barry, *Tetrahedron Lett.*, 1968, **9**, 2457–2460; (c) G. Lohaus, *Chem. Ber.*, 1967, **100**, 2719–2729; (d) S. Selvi and P. T. Perumal, *Synth. Commun.*, 2001, **31**, 2199–2202; (e) L. D. Luca, G. Giacomelli and A. Porcheddu, *J. Org. Chem.*, 2002, **67**, 6272–6274.
- E. Léonel, J. P. Paugam and J. Y. Nédélec, *J. Org. Chem.*, 1997, **62**, 7061–7064.
- For reviews, see: (a) P. Xu, W. Li, J. Xie and C. Zhu, *Acc. Chem. Res.*, 2018, **51**, 484–495; (b) J. Xie, H. Jin and A. S. K. Hashmi, *Chem. Soc. Rev.*, 2017, **46**, 5193–5203; (c) J. R. Chen, X. Q. Hu, L. Q. Lu and W. J. Xiao, *Chem. Soc. Rev.*, 2016, **45**, 2044–2056; (d) D. M. Schultz and T. P. Yoon, *Science*, 2014, **343**, 123917; (e) J. M. R. Narayanam and C. R. J. Stephenson, *Chem. Soc. Rev.*, 2011, **40**, 102–113; (f) J. Xuan and W.-J. Xiao, *Angew. Chem., Int. Ed.*, 2012, **51**, 6828–6838; (g) L. Shi and W. Xia, *Chem. Soc. Rev.*, 2012, **41**, 7687–7697; (h) C. K. Prier, D. A. Rankic and D. W. C. MacMillan, *Chem. Rev.*, 2013, **113**, 5322–5363. For recent examples, see: (i) J. B. McManus, N. P. Onuska and D. A. Nicewicz, *J. Am. Chem. Soc.*, 2018, **140**, 9056–9060; (j) N. Zhou, X. A. Yuan, Y. Zhao, J. Xie and C. Zhu, *Angew. Chem.*, 2018, **130**, 4054–4058; (k) J. Cheng, J. Xie and C. Zhu, *Chem. Commun.*, 2018, **54**, 1655–1658; (l) K. J. Romero, M. S. Galliher, D. A. Pratt and C. R. Stephenson, *Chem. Soc. Rev.*, 2018, **47**, 7851–7866; (m) A. C. Sun, E. J. McClain, J. W. Beatty and C. R. Stephenson, *Org. Lett.*, 2018, **20**, 3487–3490; (n) D. Alpers, K. P. Cole and C. R. Stephenson, *Angew. Chem., Int. Ed.*, 2018, **57**, 12167–12170; (o) S. Tripathi, R. Kapoor and L. D. S. Yadav, *Adv. Synth. Catal.*, 2018, **360**, 1407–1413; (p) S. Tripathi and L. D. S. Yadav, *New J. Chem.*, 2018, **42**, 3765–3769; (q) V. Bacauanu, S. Cardinal, M. Yamauchi, M. Kondo, D. F. Fernández, R. Remy and D. W. MacMillan, *Angew. Chem., Int. Ed.*, 2018, **57**, 12543–12548; (r) Y. Liang, X. Zhang and D. W. MacMillan, *Nature*, 2018, **559**, 83–88; (s) C. Le, T. Q. Chen, T. Liang, P. Zhang and D. W. MacMillan, *Science*, 2018, **360**, 1010–1014; (t) H. Ji, H. Q. Ni, P. Zhi, Z. W. Xi, W. Wang, J. J. Shi and Y. M. Shen, *Org. Biomol. Chem.*, 2017, **15**, 6014–6023; (u) T. K. Dey, K. Ghosh, P. Basu, R. A. Molla and S. M. Islam, *New J. Chem.*, 2018, **42**, 9168–9176.
- C. Dai, J. M. Narayanam and C. R. Stephenson, *Nat. Chem.*, 2011, **3**, 140–145.
- M. D. Konieczynska, C. Dai and C. R. J. Stephenson, *Org. Biomol. Chem.*, 2012, **10**, 4509–4511.
- (a) A. K. Yadav, V. P. Srivastava and L. D. S. Yadav, *RSC Adv.*, 2014, **4**, 4181–4186; (b) V. P. Srivastava, A. K. Yadav and L. D. S. Yadav, *Synlett*, 2014, 665–670; (c) A. K. Yadav, V. P. Srivastava and L. D. S. Yadav, *RSC Adv.*, 2014, **4**, 24498–24503.
- T. McCallum and L. Barriault, *J. Org. Chem.*, 2015, **80**, 2874–2878.
- For reviews, see: (a) M. Nolan, A. Iwaszuk, A. K. Lucid, J. J. Carey and M. Fronzi, *Adv. Mater.*, 2016, **28**, 5425–5446; (b) X. Lang, X. Chen and J. Zhao, *Chem. Soc. Rev.*, 2014, **43**, 473–486; (c) H. Kisch, *Angew. Chem., Int. Ed.*, 2013, **52**, 812–847. For recent examples, see: (d) Z. W. Xi, L. Yang, D. Y. Wang, C. D. Pu, Y. M. Shen, C. D. Wu and X. G. Peng, *J. Org. Chem.*, 2018, **83**, 11886–11895; (e) J. Tang, G. Grampp, Y. Liu, B. X. Wang, F. F. Tao, L. J. Wang, X. Z. Liang, H. Q. Xiao and Y. M. Shen, *J. Org. Chem.*, 2015, **80**, 2724–2732; (f) C. D. McTiernan, S. P. Pitre, H. Ismaili and J. C. Scaiano, *Adv. Synth. Catal.*, 2014, **356**, 2819–2824; (g) H. Zhang, Z. Zhu, Y. Wu, T. Zhao and L. Li, *Green Chem.*, 2014, **16**, 4076–4080; (h) Y. Shiraishi, H. Hirakawa, Y. Togawa and T. Hirai, *ACS Catal.*, 2014, **4**, 1642–1649; (i) H. Kominami, S. Yamamoto, K. Imamura, A. Tanaka and K. Hashimoto, *Chem. Commun.*, 2014, **50**, 4558–4560; (j) T. Hou, N. Luo, H. Li, M. Heggen, J. Lu, Y. Wang and F. Wang, *ACS Catal.*, 2017, **7**, 3850–3859; (k) D. C. Fabry, Y. A. Ho, R. Zapf, W. Tremel, M. Panthöfer, M. Rueping and T. H. Rehm, *Green Chem.*, 2017, **19**, 1911–1918; (l) Y. Cai,



- Y. Tang, L. Fan, Q. Lefebvre, H. Hou and M. Rueping, *ACS Catal.*, 2018, **8**, 9471–9476.
- 13 (a) X. Zhang, Y. Li, X. Hao, K. Jin, R. Zhang and C. Duan, *Tetrahedron*, 2018, **74**, 1742–1748; (b) D. Rackl, P. Kreitmeier and O. Reiser, *Green Chem.*, 2016, **18**, 214–219; (c) H. Takeda, M. Ohashi, Y. Goto, T. Ohsuna, T. Tani and S. Inagaki, *Adv. Funct. Mater.*, 2016, **26**, 5068–5077; (d) D. C. Fabry, M. A. Ronge and M. Rueping, *Chem. – Eur. J.*, 2015, **21**, 5350–5354; (e) W. J. Yoo and S. Kobayashi, *Green Chem.*, 2014, **16**, 2438–2442; (f) N. Priyadarshani, Y. Liang, J. Suriboot, H. S. Bazzi and D. E. Bergbreiter, *ACS Macro Lett.*, 2013, **2**, 571–574; (g) Z. Hao, S. Li, J. Sun, S. Li and F. Zhang, *Appl. Catal., B*, 2018, **237**, 366–372; (h) Y. L. Wong, J. M. Tobin, Z. Xu and F. Vilela, *J. Mater. Chem. A*, 2016, **4**, 18677–18686.
- 14 (a) F. Liu, L. Wang, Q. Sun, L. Zhu, X. Meng and F. S. Xiao, *J. Am. Chem. Soc.*, 2012, **134**, 16948–16950; (b) Y. Zhang, S. Wei, F. Liu, Y. Dua, S. Liu, Y. Ji, T. Yokoi, T. Tatsumi and F.-S. Xiao, *Nano Today*, 2009, **4**, 135–142.
- 15 F. Peng, P. Zhi, H. Ji, H. Zhao, F. Y. Kong, X. Z. Liang and Y. M. Shen, *RSC Adv.*, 2017, **7**, 19948–19953.
- 16 Z. Zhao, Z. Peng, Y. Zhao, H. Liu, C. Li and J. Zhao, *J. Org. Chem.*, 2017, **82**, 11848–11853.
- 17 C. Ramalingan and Y. T. Park, *J. Org. Chem.*, 2007, **72**, 4536–4538.
- 18 J. Zhang, Y. Ma and Y. Ma, *Eur. J. Org. Chem.*, 2018, 1720–1725.
- 19 S. Stavberand and M. Zupan, *J. Org. Chem.*, 1985, **50**, 3609–3612.
- 20 Y. Peng, H. Liu, M. Tang, L. Cai and V. Pike, *Chin. J. Chem.*, 2009, **27**, 1339–1344.
- 21 T. K. Macklin and V. Snieckus, *Org. Lett.*, 2005, **7**, 2519–2522.
- 22 L. Wang, Y. Wang, J. Shen, Q. Chen and M. Y. He, *Org. Biomol. Chem.*, 2018, **16**, 4816–4820.
- 23 S. Ushijima, K. Moriyama and H. Togo, *Tetrahedron*, 2011, **67**, 958–964.
- 24 L. Buzzetti, A. Prieto, S. R. Roy and P. Melchiorre, *Angew. Chem.*, 2017, **129**, 15235–15239.
- 25 D. Zhang, Y. Huang, E. Zhang, R. Yi, C. Chen, L. Yu and Q. Xu, *Adv. Synth. Catal.*, 2018, **360**, 784–790.
- 26 M. D. Konieczynska, C. Dai and C. R. Stephenson, *Org. Biomol. Chem.*, 2012, **10**, 4509–4511.
- 27 Y. D. Park, J. J. Kim, H. K. Kim, S. D. Cho, Y. J. Kang, K. H. Park and Y. J. Yoon, *Synth. Commun.*, 2005, **35**, 371–378.